Filtering Out Photonic Fock States

Kaoru Sanaka,[1,*] Kevin J. Resch,[1,†] and Anton Zeilinger[1,2]

[1]*Institut für Experimentalphysik, Universität Wien, Boltzmanngasse 5, 1090 Vienna, Austria*

[2]*Institut für Quantenoptik und Quanteninformation, Österreichische Akademie der Wissenschaften, Boltzmanngasse 3, 1090 Vienna, Austria*

(Received 19 March 2005; published 27 February 2006)

Unprecedented optical nonlinearities can be generated probabilistically in simple linear-optical networks conditioned on specific measurement outcomes. We describe a highly controllable quantum filter for photon number states, which takes advantage of such a measurement-induced amplitude nonlinearity. The basis for this filter is multiphoton nonclassical interference which we demonstrate for one- and two-photon states over a wide range of beam splitter reflectivities. Specifically, we show that the transmission probability, conditional on a specific measurement outcome, can be larger for a two-photon state than a one-photon state; this is not possible with linear optics alone.

DOI: 10.1103/PhysRevLett.96.083601 PACS numbers: 42.50.Ar, 03.67.Lx, 42.50.Dv

Experimental quantum optics faces considerable challenges in the controlled creation, detection, and manipulation of light. Without strong photon-photon interactions or optical nonlinearities, it is very difficult to arbitrarily manipulate the distribution of photons within an optical beam [1]. A great deal of effort has been concentrated on this problem since it is also a major hurdle for optical quantum computation. With that purpose in mind, it was found that huge probabilistic nonlinearities can occur in *linear*-optical systems supplemented by extra ''ancilla'' photons and projective measurement [2]. The nonlinearities produced by this method are so strong that pairs of photons effectively interact. Experimental demonstrations of dispersive or phase nonlinearities [3] and quantum logic gates [4,5] have been performed based on these techniques [6]. These linear optics methods create, in general, a complex mix of phase and amplitude nonlinearities. Amplitude nonlinearities, and absorption in general, are undesirable for quantum computation since they can result in information loss. However, amplitude nonlinearities are potentially powerful for controlling the mode properties and photon statistics of weak light beams [7]. Measurement-induced amplitude nonlinearities build on previous techniques using photon addition or subtraction and ''quantum scissors'' which use conditional measurements to modify the quantum state of a light beam [8]. In the present work, we demonstrate a measurement-induced amplitude nonlinearity that can be used to completely remove a single component from a superposition of photon number states. This constitutes a quantum filter that acts as a highly controllable n-photon absorber [9].

Consider the optical schematic shown in Fig. 1. An n-photon state is incident in mode 1 and an ancilla photon is incident in mode 2. The beam splitter implements the linear-optical transformation $a_1 \rightarrow ta_3 + ra_4$ and $a_2 \rightarrow ra_3 - ta_4$, where $r(t)$ are real reflection (transmission) amplitudes, and a_i is the lowering operator for mode i. If the photons are indistinguishable, the amplitude to find a single (i.e., one and only one) photon in mode 3, and hence n photons in mode 4, is given by the expression $A_{NL}(n) = \sqrt{R}^{n-1}[R - n(1 - R)]$, where $R = r^2$ is the reflectivity of the beam splitter [3,10]. This amplitude is a result of the quantum interference between the two paths leading to a single photon in mode 3. Either all $n + 1$ photons reflect at the beam splitter, or the ancilla and one photon from the n-photon state are transmitted and the remaining $n - 1$ photons are reflected. The second process can occur n different ways and is therefore weighted more heavily for higher n. Squaring the amplitude, we obtain the probability to find a single photon in mode 3 and n photons in mode 4,

$$P_{NL} = R^{n-1}[R - n(1 - R)]^2. \quad (1)$$

We define P_{NL} as the conditional transmission probability for the quantum filter.

We consider a general pure state in mode 1, $|\psi\rangle_1 = \sum_{n=0}^{\infty} c_n|n\rangle_1$, in which the complex amplitudes, c_n, satisfy $\sum_{n=0}^{\infty} |c_n|^2 = 1$. A single ancilla photon is incident in mode 2. Following the transformation implemented by the beam splitter, measurement of a single photon in

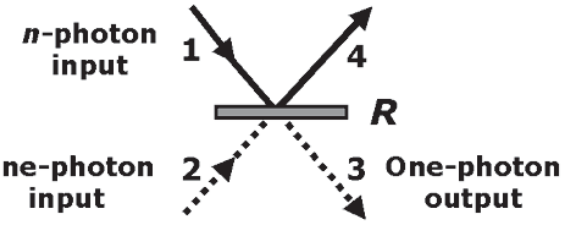

FIG. 1. Schematic setup for the quantum filter. An n-photon state in mode 1 and ancilla photon in mode 2 are incident on a beam splitter with reflectivity, R. The probability to find a single (i.e., one and only one) photon in mode 3, and hence n-photons in mode 4, is $P_{NL} = R^{n-1}[R - (1 - R)n]^2$. When $R = n/(n + 1)$, one never finds a single photon in the output mode 3. By the linearity of quantum mechanics, if the input state had contained a superposition of photon number states, and a single photon was found in mode 3, the n-photon component would be completely removed from the output state.

 © 2006 The American Physical Society

mode 3 yields some information about the remaining number of photons in mode 4. This information is due to dependence of the amplitude, A_{NL}, on n and leads to the nonunitary transformation $|\psi\rangle_1 \rightarrow |\psi'\rangle_4 = \mathcal{N}\sum_{n=0}^{\infty} \times \sqrt{R}^{n-1}[R - n(1-R)]c_n|n\rangle_4$, where the normalization coefficient, $\mathcal{N}$, is a function of c_n and R.

The most important consequence for this work is that for $R = n/(n+1)$, $P_{NL} = 0$. For this specific R, theory predicts that when an n-photon state enters the filter, a single photon never emerges in mode 3. By the linearity of quantum mechanics, if the input state was a superposition of number states containing $|n\rangle$ and a single photon was found in mode 3, the output state no longer contains $|n\rangle$. In this sense, the device acts as a conditional n-photon absorber. The transformation implemented by the filter has other important features. It is diagonal in the Fock state basis and therefore only those Fock states contained in the initial state can be in the final state. Furthermore, the dependence on a specific measurement outcome makes the transformation both probabilistic and, in general, not unitary.

The filter relies on quantum interference and thus indistinguishability plays a central role. If a time delay is introduced between the ancilla and the n-photon state such that they no longer arrive at the beam splitter simultaneously, then the interference giving rise to Eq. (1) is destroyed. Instead, a classical mixture arises because either all of the photons are reflected and the output photons remain in a single pulse, or the ancilla and an input photon are exchanged by transmission through the beam splitter and the output consists of $n-1$ photons in one pulse and a single photon in a temporally separate pulse. The probability for this classical mixture to arise is $P_{CM} = R^{n+1} + R^{n-1}(1-R)^2 n$. The time delay is controlled in our experiment to compare the evolution when interference occurs to those cases where it does not.

For a single input photon (the $n = 1$ case), this interference was first demonstrated by Hong, Ou, and Mandel (HOM). In their experiment, two photons entered a $R = 1/2$ beam splitter from different input ports [11]. If there is no which-path information, the two paths leading to a single photon in each output mode interfere completely destructively. As a result the photons always emerge as pairs and never as a single photon, leading to a drop in the coincidence detection rate between the two output ports. The depth of an interference dip is typically characterized by the visibility: $V = (P_{CM} - P_{NL})/P_{CM}$, which is a standard measure of the contrast of the interference. For HOM interference, the visibility can range from 0%, in the case where there is no interference, to 100%, in the case where there is perfect destructive interference. Inverting the expression for the visibility gives $P_{NL} = P_{CM}(1-V)$, which relates the conditional transmission probabilities characterizing the quantum filter from the experimentally measured visibilities. For a fixed number of input photons, n, we can use the expressions for P_{NL} and P_{CM} to obtain the expected visibility, $V = [(R-1)^2 + R^2/n]^{-1} - n$.

Practical implementation of this quantum filter and scalable linear optics quantum gates [4,5] share the same technological difficulties: widely available single-photon counting detectors cannot distinguish between one photon and two [12], down-conversion is a probabilistic instead of deterministic emitter of photon pairs, and photon loss (or detector inefficiency) introduces errors. All of these effects have the undesirable characteristics of introducing photon number uncertainty into the experiment. Nevertheless, even with these constraints, it is still possible to compare the behavior of the filter with interference to those cases without when the number of input photons is certain. This is accomplished through multiphoton coincidence detection which rejects those cases where the source did not emit photons or photons were lost and not detected. Developments in source and detector technology necessary for optical quantum computation are also required for this quantum filter to act on input states with uncertain photon number.

The experimental setup is shown in Fig. 2. Frequency-doubled pulses from a mode-locked Ti:sapphire laser (394.5 nm central wavelength, 200 fs pulse duration, and 76 MHz repetition rate) pass twice through a type-II phase-matched barium-borate (BBO) crystal. The crystal was cut to produce polarization-entangled pairs via parametric down-conversion [13], but the polarization entanglement did not play a role here. The first polarizing beam splitter [PBS, Fig. 2(c)] projects out product states for further participation in the experiment. Recall that a PBS transmits horizontally polarized light and reflects vertically polarized light. In those cases where we used a single-photon input state, we employed a single pair of down-conversion photons [Fig. 2(a)]. When we used a two-photon input state (the $n = 2$ case) in addition to the ancilla, we used two independent down-conversion pairs [Fig. 2(b)]. A horizontally polarized two-photon state was probabilistically created from the forward down-conversion pair using a 50/50 fiber beam splitter. To investigate the full range of behavior of the quantum filter in a single experimental setup, we constructed a variable beam splitter (VBS) using two PBSs and a half-wave plate (HWP). The angle between the HWP fast axis and horizontal, θ, can be changed to give $R = \sin^2 2\theta$ [5,14]. Photodetection is carried out by the single-photon counting detectors D_1, D_2, D_3, and D_4. Fourfold detection probabilities are similar to those described in Ref. [3]. In the $n = 1$ case, the twofold coincidence events between detectors D_2 and D_3 were measured. In the $n = 2$ case, we measured fourfold coincidences between detectors D_1–D_4 with detectors D_3 and D_4 acting as a cascaded two-photon detector.

For the experiment, we control the relative delay, and hence the degree of distinguishability, between the ancilla and one- or two-photon state into the VBS. This is ac-

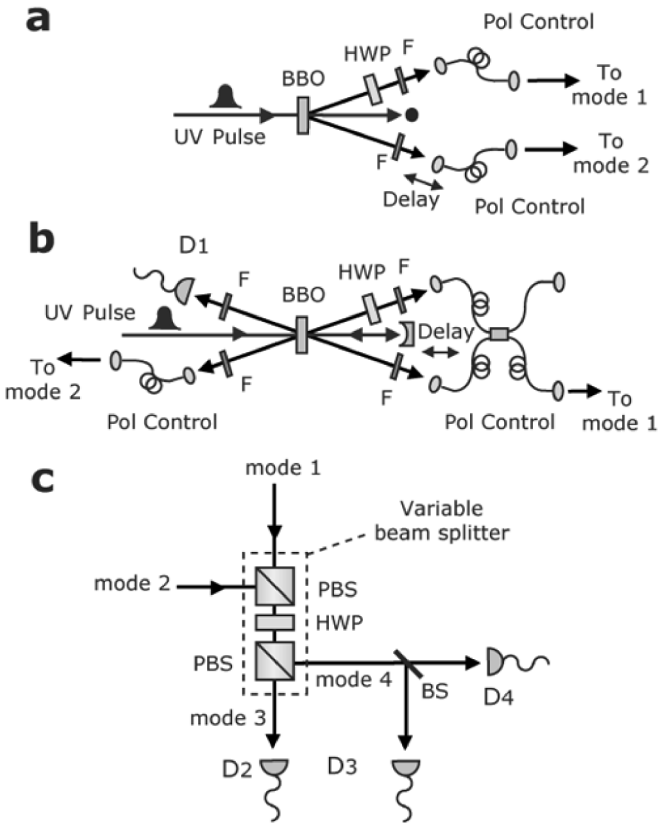

FIG. 2. Experimental setup for the demonstration of a quantum filter. Input states containing one or two photons are produced using parametric down-conversion in a type-II phase-matched 2-mm BBO crystal pumped by ultraviolet laser pulses. Interference filters (F) select light with a center wavelength of 789 nm and bandwidth of 4 nm. (a) In the $n = 1$ case, the input photon and ancilla photon originate from the same down-conversion pair. Polarization controllers (Pol Control) compensate unwanted polarization rotations in the optical fibers. (b) In the $n = 2$ case, the two input photons came from one down-conversion pair on the forward pass of the pump. These photons were probabilistically combined into the same optical mode using a fiber beam splitter. This produces a horizontally polarized two-photon state. The vertically polarized ancilla is produced in a second down-conversion pair on the backward pass of the pump heralded by a detection event at D_1. The one- or two-photon states are contained in mode 1 and the ancilla photon in mode 2. (c) The photons were combined in a variable-reflectivity beam splitter constructed using two polarizing beam splitters (PBSs) and a half-wave plate (HWP). Their relative times of arrival were controlled by the delays on the fiber coupler and pump mirror. In output mode 3, a click at detector D_2 is required for the quantum filter to implement the desired transformation. In the $n = 1$ case, the output photons were measured at detector D_3, while in the $n = 2$ case photon pairs were detected by the cascaded detector pair D_3 and D_4.

complished either by using the fiber coupler in mode 2 in the $n = 1$ case, or by controlling the time delay of the pump laser on its second pass through the BBO crystal in the $n = 2$ case. The twofold or fourfold coincidences were recorded as a function of these delays for different R values. Raw data accumulated in the experiment are shown in Figs. 3(a) and 3(b) where the solid lines are Gaussian fits.

Figure 3(a) shows the twofold coincidence counts accumulated in 10 s ($n = 1$ case). All cases measured in this configuration show a drop in the coincidence rate near zero relative delay. In this configuration, the maximum measured visibility of $(83 \pm 1)\%$ was obtained when $R = 1/2$. Visibilities for other measured cases and the theoretical prediction are summarized as the open data points and curve in Fig. 3(c). Note that the visibility is expected to drop to zero as R is raised or lowered to either extreme.

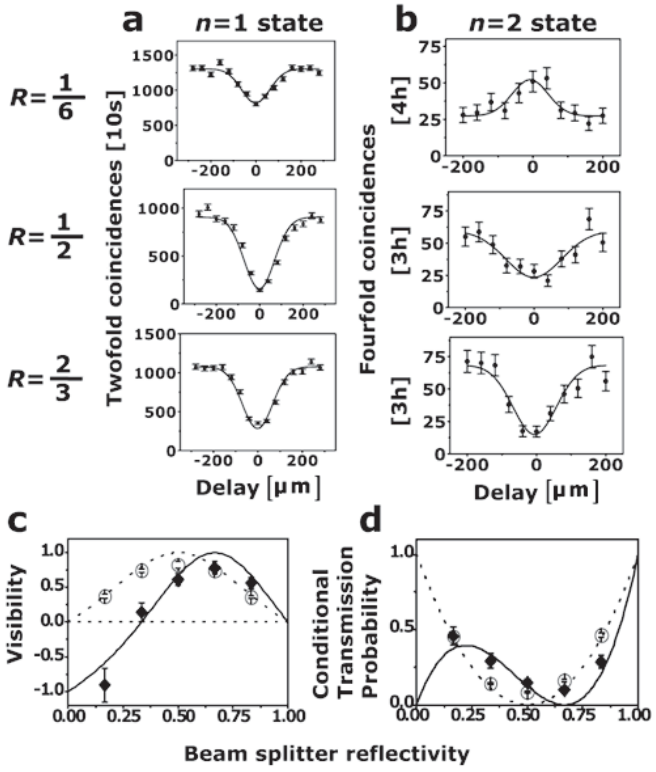

FIG. 3. Experimental results for one- and two-photon input states. (a) The twofold coincidences for the $n = 1$ configuration [Fig. 2(a)] between detectors D_2 and D_3 are shown as a function of the relative delay introduced by the fiber coupler. Solid lines show Gaussian fits to the data. All cases show a decrease in the coincidence rate with a maximum measured visibility of $(83 \pm 1)\%$ for $R = 1/2$. (b) The fourfold coincidences as a function of delay for the $n = 2$ source configuration [Fig. 2(b)] for the same R values. In this case, the maximum visibility was measured to be $(78 \pm 5)\%$ at $R = 2/3$ not $1/2$. The experimental data for $R = 1/6$ show an increase in coincidence rate at zero delay. (c) All experimentally measured visibilities are shown as a function of the R for $n = 1$ (open circles, dotted line theory) and $n = 2$ (solid diamonds, solid line theory) input states. (d) Conditional transmission probabilities inferred from the experimental data are shown for both the $n = 1$ (open circles, dotted line theory) and $n = 2$ (solid diamond, straight line theory) cases for different R settings.

This $n = 1$ behavior is well known [11] and is starkly contrasted by that of the $n = 2$ case. Figure 3(b) shows the fourfold coincidences accumulated in either 3 or 4 h between the detectors D_1–D_4 for the two-photon input state and source configuration in Fig. 2(b). The maximum measured visibility of $(78 \pm 5)\%$ no longer occurs when $R = 1/2$ but rather $R = 2/3$. This shift in the maximum visibility is explained by our theory, which predicts that the visibility reaches a maximum of 100% at $R = 2/3$. The experimental data measured for $R = 1/6$ show an *increased* coincidence rate near zero delay with a visibility of $(-93 \pm 26)\%$ where the sign change indicates constructive rather than destructive interference. The change in sign of the visibility is not a feature of original HOM nonclassical interference. However, this sign change is predicted by our theory and is expected for all $n \geq 2$ when $R < (n - 1)/(n + 1)$.

The experimentally measured visibilities provide the characteristics of the quantum filter. For very large delays, we assume our classical mixture model adequately describes the outcome probabilities and we use the experimentally measured visibilities to extract the conditional transmission probability P_{NL}. Figure 3(d) displays the results for $n = 1$ (open circles, dotted line theory) and $n = 2$ (solid diamonds, straight line theory). We have good agreement between experiment and theory here for the characteristics of the filter. Discrepancies near the minimum conditional transmission probability are due to sensitivity to mode mismatch. Improvements in source characteristics, specifically removing the distinguishing information between independent down-conversion pairs [15], and using waveguided optics are expected to significantly improve the interference contrast [16]. Nevertheless, we clearly see that in the experiment there are R values where the attenuation for the two-photon state is larger than for the one-photon state and vice versa. For example, when R was set to $1/3$, the extracted conditional transmission probability for the one-photon state was $(14.1 \pm 0.7)\%$, while for the two-photon state it was $(29.2 \pm 4.9)\%$. In a passive linear-optical system, where photons are absorbed in an uncorrelated way, a higher photon number state cannot be attenuated less than a lower photon number state. Thus our filter implements a nonlinear-optical absorption process.

The absence of strong interactions and optical nonlinearities is restrictive in quantum optics. Measurement-induced optical nonlinearities, which were originally proposed in the context of optical quantum computation [2], offer such strong nonlinearities that individual photons can effectively interact. We have implemented the fundamental elements of a quantum filter for photon Fock states based on a measurement-induced absorptive nonlinearity. Specifically, we have demonstrated the dramatically different underlying nonclassical interference behavior for one- and two-photon input states. This absorptive nonlinearity promises to be a powerful additional tool for controlling the properties of light a few photons at a time.

We are grateful for the technical assistance of Rupert Ursin and stimulating discussions with Gabriel Molina-Terriza. This work was supported by the Austrian Science Foundation (FWF), Projects No. M666 and No. SFB 015 P06, NSERC, and the European Commission, Contract No. IST-2001-38864.

*Present address: E. L. Ginzton Laboratory, Stanford University, Stanford, CA 94305, USA.
†Present address: Department of Physics, University of Queensland, Brisbane QLD 4072, Australia.

[1] G. J. Milburn, Phys. Rev. Lett. **62**, 2124 (1989); I. L Chuang and Y. Yamamoto, Phys. Rev. A **52**, 3489 (1995).
[2] E. Knill, R. Laflamme, and G. J. Milburn, Nature (London) **409**, 46 (2001).
[3] K. Sanaka *et al.*, Phys. Rev. Lett. **92**, 017902 (2004).
[4] T. B. Pittman, B. C. Jacobs, and J. D. Franson, Phys. Rev. A **64**, 062311 (2001); S. Gasparoni *et al.*, Phys. Rev. Lett. **93**, 020504 (2004).
[5] J. L. O'Brien *et al.*, Nature (London) **426**, 264 (2003).
[6] T. Rudolph and J.-W. Pan, quant-ph/0108056; T. C. Ralph *et al.*, Phys. Rev. A **65**, 012314 (2002); M. Koashi, T. Yamamoto, and N. Imoto, Phys. Rev. A **63**, 030301(R) (2001); H. F. Hofmann and S. Takeuchi, Phys. Rev. A **66**, 024308 (2002).
[7] B. M. Escher *et al.*, Phys. Rev. A **70**, 025801 (2004); K. J. Resch, Phys. Rev. A **70**, 051803(R) (2004); K. Sanaka, Phys. Rev. A **71**, 021801(R) (2005).
[8] G. T. Foster *et al.*, Phys. Rev. Lett. **85**, 3149 (2000); K. J. Resch, J. S. Lundeen, and A. M. Steinberg, Phys. Rev. Lett. **88**, 113601 (2002); A. I. Lvovsky and J. Mlynek, Phys. Rev. Lett. **88**, 250401 (2002); J. Wenger, R. Tualle-Brouri, and P. Grangier, Phys. Rev. Lett. **92**, 153601 (2004); A. Zavatta, S. Viciani, and M. Bellini, Science **306**, 660 (2004).
[9] H. F. Hofmann and S. Takeuchi, Phys. Rev. Lett. **88**, 147901 (2002); X. B. Zou, K. Pahlke, and W. Mathis, Phys. Rev. A **66**, 064302 (2002); A. Grudka and A. Wojcik, Phys. Rev. A **66**, 064303 (2002).
[10] H. F. Hofmann and S. Takeuchi, quant-ph/0204045.
[11] C. K. Hong, Z. Y. Ou, and L. Mandel, Phys. Rev. Lett. **59**, 2044 (1987).
[12] K. J. Resch, J. S. Lundeen, and A. M. Steinberg, Phys. Rev. A **63**, 020102(R) (2001).
[13] P. G. Kwiat *et al.*, Phys. Rev. Lett. **75**, 4337 (1995).
[14] M. Mohseni *et al.*, Phys. Rev. Lett. **91**, 187903 (2003).
[15] W. P. Grice, A. B. U. Ren, and I. A. Walmsley, Phys. Rev. A **64**, 063815 (2001).
[16] T. B. Pittman and J. D. Franson, Phys. Rev. Lett. **90**, 240401 (2003).